Laser and Particle Beams (2001), *19*, 201–204. Printed in the USA.

Advanced instrumentation for spectral and spatial investigations of high-order laser harmonics

LUCA POLETTO, GIUSEPPE TONDELLO, AND PAOLO VILLORESI

INFM—Istituto Nazionale per la Fisica della Materia, Department of Electronics and Informatics, University of Padova, Padova, Italy

(RECEIVED 30 November 2000; ACCEPTED 5 February 2001)

Abstract

We report on the design and characterization of a grazing-incidence flat-field spectrograph that allows simultaneously the measurement of spectrum, beam divergence, and absolute flux of EUV and soft X-ray radiation for a beam of high-order laser harmonics generated by the interaction between an ultrashort femtosecond laser pulse and a gas jet. The instrument seems a very powerful tool for the understanding of the generation process.

1. INTRODUCTION

Since their experimental discovery (Carman *et al.*, 1981), high-order harmonics obtained by intense ultrashort pulsed lasers focused onto a gas jet has been emerging as a new field of nonlinear optics with very attractive characteristics and unique properties, such as high brightness, good temporal and spatial coherence, and extremely short pulse duration obtained in a table-top apparatus (Ditmire *et al.*, 1996; Glover *et al.*, 1996; Protopapas *et al.*, 1997). Thanks to these unique features, high-order harmonic sources are requested in a number of applications in physics, chemistry, and biochemistry, for example, in high time-resolution pump and probe experiments or in experiments requiring high instantaneous power in ionization or excitation interactions. The high-order harmonics spectrum is a sequence of peaks corresponding to the odd harmonics of the laser frequency, with a vast plateau characterizing the intensity distribution of the peaks, whose extension is related to pulse intensity (Salières *et al.*, 1998). The availability of extremely short pulse duration solid-state lasers (Nisoli *et al.*, 1996, 1997) has allowed the efficient generation of harmonic pulses with duration in the range 5–30 fs and the emission of coherent radiation down to the *water window* spectral region (2.3–4.4 nm) (Spielmann *et al.*, 1997), still using as a source a table-top apparatus.

The study of high-order harmonics generated in few-optical-cycle pulses deserves much attention (Altucci *et al.*, 2000*a*, Villoresi *et al.*, 2000). A large sensitivity to both laser parameters and target conditions is expected, so the measurements of the more relevant characteristics of the harmonic beam have to be done simultaneously in order to gain an insight into the generation process within controlled conditions. The main measurements to be done are both those in the spectral domain, as the spectral distribution, the relative spectral intensity, the linewidth of the harmonic lines, and the wavelength shift occurring for different conditions (Altucci *et al.*, 2000*b*), and the beam divergence, resolved in generation position and harmonic order, as well as general features as the global conversion efficiency of the generation process in the EUV and soft X-ray spectral regions and the pulse-to-pulse variation due to the fluctuation of the pulse carrier phase (Priori *et al.*, 2000). In this spirit, we have realized a grazing-incidence flat-field spectrograph able to measure simultaneously spectral features, angular divergence, and absolute photon flux, with also the possibility of following the dynamic evolution of the high-order harmonic spectrum in the single-shot mode. The design combines an advanced optical setup with an EUV-sensitive bidimensional detector. The instrument is presented in detail in Section 2; some experimental results are then shown in Section 3.

2. GRAZING-INCIDENCE FLAT-FIELD SPECTROGRAPH

The acquisition of EUV and soft X-ray high-order harmonics requires wide-band grazing-incidence grating spectrographs. In case of the classical Rowland mounting with spherical gratings, the spectral focal curve is a cylindrical

Address correspondence and reprint requests to: Luca Poletto, INFM—Istituto Nazionale per la Fisica della Materia, Department of Electronics and Informatics, University of Padova, via Gradenigo 6/A—35131 Padova, Italy. E-mail: poletto@dei.unipd.it

surface with diameter equal to the grating radius (the so-called Rowland cylinder); an extended spectrum is acquired by moving the detector tangent to the Rowland circle, making it impossible to have simultaneously a wide-band spectral region on the detector (Samson & Ederer, 1998). On the contrary, an almost flat focal surface at near normal incidence on the detector is obtained by using SVLS gratings, in which the groove spacing changes on the surface following a polynomial law (Kita *et al.*, 1983; Nakano *et al.*, 1984): in such a system the aberrations can be controlled by the ruling parameters for groove space variation. By choosing a proper distribution of the line spacing, the spectral focal curve can be brought to be almost straight, fitting well the detector plane (Harada *et al.*, 1999): in this case, a wide spectral interval can be obtained although on a single acquisition.

The flux collected by the grating is increased by focusing the radiation coming from the source on the entrance slit of the spectrograph: this is usually performed by a toroidal mirror mounted between the source and the entrance slit, with its tangential focus on the slit itself. Furthermore, the mirror can compensate the grating astigmatism due to the grazing-incidence mounting. In fact, a grazing-incidence spherical grating does not provide practically any focusing capability in a plane perpendicular to the dispersion one. An emitting point placed on the entrance slit is acquired on the focal plane as a long and slightly curved line (Poletto, 2000). In case of Rowland mountings, the length of the spectrograph exit arm changes quickly with the wavelength as the cosine of the diffraction angle, so it is impossible to correct for the astigmatism in an extended spectral region. In fact, the toroidal mirror has a variable exit arm giving large defocusing when moving the detector far from the stigmatic wavelength (Tondello, 1979; Chrisp, 1983). On the contrary, the exit arm of an SVLS grating is almost constant also in an extended spectral region, making easier to correct for the astigmatism in the whole region to be acquired. This is performed by placing the sagittal focus of the toroidal mirror on the focal plane of the spectrograph (Choi *et al.*, 1997). If the stigmaticity is not required, the sagittal focus can be put in front of the grating focus. In this way, a residual astigmatism is obtained and the length of the spectral lines on the spectrum is proportional to the sagittal angular divergence of the beam (Poletto, 2001). So, an SVLS grating coupled with a toroidal mirror and a suitable bidimensional detector results in a spectrograph able to measure simultaneously both spectral and spatial features of the high-order harmonic spectrum in a wide spectral region. A schematic view of the optical configuration is shown in Figure 1.

The SVLS grating is manufactured by Hitachi. It is gold coated, with 1200 lines/mm central groove density, 5649 mm radius, 87° incidence angle and 237 mm entrance arm. The parameters for groove space variation have been chosen to give an almost flat spectral focal curve in the 5–40 nm region, located at 235 mm from the grating vertex, and parallel to the normal of the grating in its vertex. In the 6–33 nm region, the maximum deviation between the actual curve and the detector plane is less than 0.5 mm, so the residual defocusing is almost negligible. The toroidal mirror focuses the radiation emitted by the laser–gas interaction point on the grating entrance plane. It is platinum coated, with 6500-mm tangential radius and 14.7-mm sagittal radius, mounted at an 86° incidence angle. Its tangential radius has been chosen so as to work with unity magnification in the tangential plane (i.e., in on-Rowland mounting with equal entrance and exit arms). This minimizes the tangential aberrations on the grating entrance plane. The sagittal focus lie before the grating focal plane, so the height of the spectral lines on the detector is proportional to the sagittal beam divergence. Note that the grating works slitless thanks both to the limited size of the emitting source, which has been estimated to be of the order of 15 μm at full-width-at-half-maximum (FWHM), and to the low tangential aberrations of the toroidal mirror on the grating entrance plane, which have been calculated to be about 6 μm at FWHM.

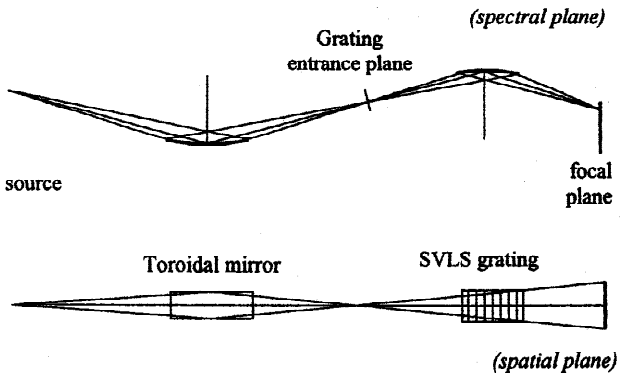

Fig. 1. Optical design of the spectrograph. The top view refers to the plane of dispersion (spectral plane) and the bottom one to the plane perpendicular to the plane of dispersion (spatial plane).

The bidimensional detector is a single-stage 40 mm MCP open intensifier manufactured by Photek with a magnesium fluoride photocathode. Input photons are converted by the photocathode into electrons that are amplified into the microchannels by an applied voltage of 1000 V at maximum. The electron clouds at the MCP output are accelerated onto a phosphor screen by a 4500-V voltage drop. The resulting image is optically coupled by an objective to a cooled CCD camera with low read-out noise manufactured by Hamamatsu. The CCD format is 1280 $\times$ 1024 pixels with a pixel size of 6.7 $\times$ 6.7 μm^2 and 10 Hz maximum frame rate. It is then possible to follow the dynamic evolution of the spectral features in the single-shot mode at 10 shots/s. The plate factor when the 40-mm phosphor screen diameter is projected on the CCD 1280 pixel long side is about 31 μm/pixel: the plate factor is shown in Figure 2. The sensitive area of the detector covers only a portion of the spectral range, so it is necessary to move the intensifier along the focal curve to scan the whole 5–40 nm spectrum. To perform this, the detector is mounted on an x–y linear drive and a z rotator and con-

https://doi.org/10.1017/S0263034601192050 Published online by Cambridge University Press

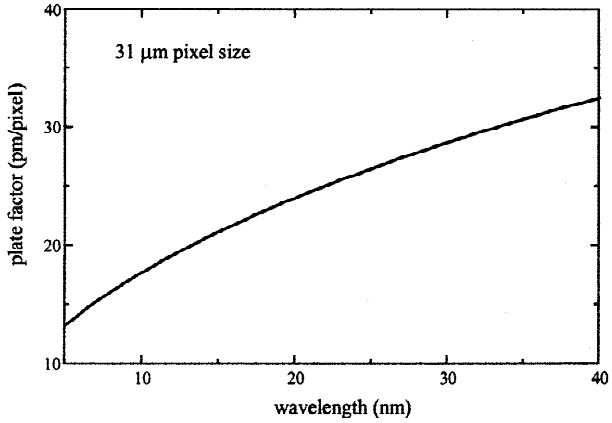

Fig. 2. Plate factor with 31-μm pixel size.

nected to the body of the spectrograph by a bellows: two different positions are required for the whole 5–40 region.

Finally, the laser source of our experiment is a Ti:sapphire system with up to 0.8-mJ energy 30-fs pulses centered at 795 nm at 1 kHz repetition rate; sub-10 fs pulses are generated by the hollow fiber compression technique (Nisoli *et al.*, 1997). The laser beam is focused by a 25-cm focal length silver mirror through a 0.5-mm-thick fused-silica window into the laser–gas interaction chamber. The gas sample is injected into the interaction chamber by a pulsed electromagnetic valve operating with about 400 μs opening time and producing gas jets having diameter at the nozzle of 0.8 mm.

A schematic view of the spectrograph with the laser-gas interaction chamber and the detector is shown in Figure 3. A differential pumping unit guarantees a pressure inside the spectrograph of the order of $7 \cdot 10^{-6}$ mbar, which is safe for the MCP detector, when operating the emitting valve at 10 Hz with a pressure inside the interaction chamber of the order of 10^{-3} mbar.

The FWHM spectral aberrations on the detector plane have been calculated for a source with parameters matching the expected characteristics of the high-order harmonic emission, that is, Gaussian distribution of the emitted rays, 15-μm size at FWHM and 10-mrad angular aperture. The aberrations are within the 31-μm pixel size in the whole 5–35 nm region and increase up to 50–55 μm at the extreme wavelengths of the range where the spectral focal curve does not match at the best detector plane. The actual spectral aberrations have been measured using the spectra emitted by a microfocus soft X-ray source with different anodes in the 7–25 nm region: by measuring the relative broadening of the emission lines at I and II diffracted orders, the residual FWHM spectral aberrations have been evaluated to be around 10–15 μm, in good agreement with the calculations.

To measure the absolute photon flux and then the conversion efficiency of the harmonic generation process, the absolute response of the system was measured in the 5–25 nm spectral region (Poletto *et al.*, 1999). The response of the whole system, which includes mirror reflectivity, grating diffraction efficiency, and detector efficiency with 950 V applied to the MCP, ranges from 0.05 DU per source photon at 5 and 25 nm to 0.2 DU per photon in the 9–11 nm region (DU is the digital unit read from the CCD analog-to-digital converter). Defining the minimum detectable signal as the photon flux necessary to give a signal comparable to the rms noise of the CCD camera, that is, about 3.5 DU rms, the minimum flux is about 50 source photons at 6.7 nm, 20 photons at 10 nm, and 90 photons at 25 nm, making the system very sensitive.

Finally, the relation between line height and sagittal divergence of the high-order harmonic emission is shown in Figure 4, as obtained by a detailed ray-tracing of the instrument.

3. EXPERIMENTAL RESULTS

As an example of application, a spectrum in He with 30 fs laser pulses and the detector positioned to acquire the 5–37 nm region is shown in Figure 5. The wavelength scale is on the horizontal axis increasing toward the right

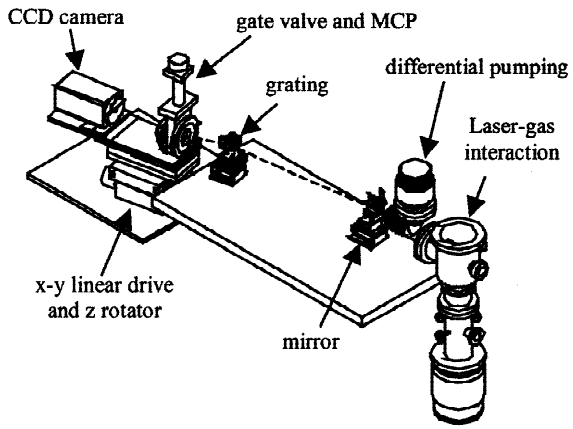

Fig. 3. Schematic view of the whole spectrograph.

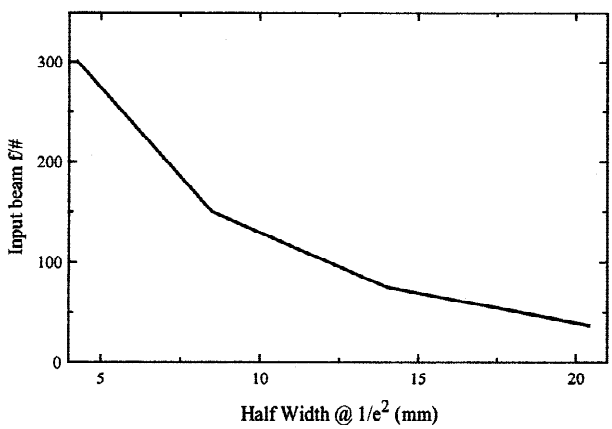

Fig. 4. Relation between line height and beam sagittal divergence.

https://doi.org/10.1017/S0263034601192050 Published online by Cambridge University Press

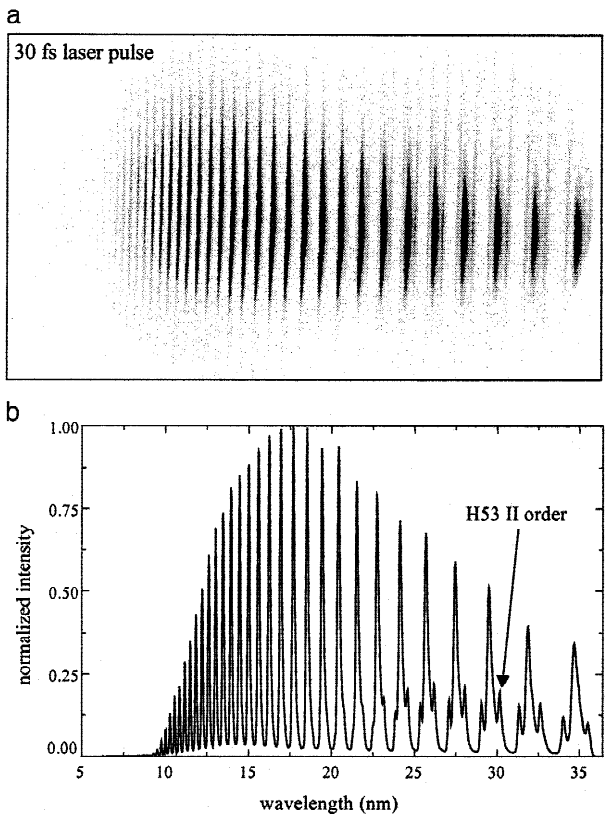

Fig. 5. High-order harmonic spectrum in He: (a) image on the CCD in the 6–37 nm region with 30-fs laser pulses, 390-μJ laser energy, valve at 10 Hz, 5-s integration time; (b) horizontal plot across the spectrum. The arrow indicates the II diffracted order of H53.

side of the image; the out-of-focus spatial distribution in the sagittal plane is instead on the vertical axis. Note the border of the circular phosphor screen in the right side of the image. The spectral features clearly visible around the harmonics at high wavelengths are II diffracted orders. Being the spectrum formed only of odd-order harmonics, the II orders are separated in the wavelength scale from the I versions; furthermore, they are clearly distinguishable because of the lower divergences of harmonics at long wavelengths. The total number of photons emitted in the 7–25 nm region is about $3 \cdot 10^7$ photons per shot, resulting in a global EUV conversion efficiency of $8.8 \cdot 10^{-7}$.

4. CONCLUSIONS

The design and performance of a spectroscopic instrument able to measure simultaneously special features, angular divergence, and conversion efficiency of high-order harmonics generated by an ultrashort pulsed laser focused onto a gas jet have been presented. It combines an advanced optical setup with an EUV-sensitive bidimensional detector.

A flat focal surface, although in grazing incidence, is obtained by using a SVLS grating optimized in the 5–40 nm region. The flux collected by the grating is increased by using a toroidal mirror with its tangential focus on the grating entrance plane; the mirror does not compensate for the grating astigmatism, so the length of the spectral lines on the spectrum is proportional to the sagittal angular divergence of the high-order harmonic emission. The system has been absolutely calibrated, so it is possible to measure the photons flux emitted by the EUV source. Furthermore, the sensitivity is very high, making the system able to work in the single-shot operation. At the present, the instrument has been intensively used for diagnostics of high-order harmonic spectra.

ACKNOWLEDGMENTS

The authors would like to thank Dr. G. Naletto and Mr. P. Zambolin for help in the realization of the spectrograph. This study was partially supported within the framework of the INFM (Istituto Nazionale per la Fisica della Materia) under the project "Femtosecond soft X-ray generation by high-energy laser pulses," in which Politecnico of Milano and Universities of Padova and Napoli are involved.

REFERENCES

Altucci, C. *et al.* (2000*a*). *J. Opt. A: Pure Appl. Opt.* **2**, 289.
Altucci, C. *et al.* (2000*b*). *Phys. Rev. A* **61**, 021801.
Carman, R.L. *et al.* (1981). *Phys. Rev. A* **24**, 2649.
Choi, I.W. *et al.* (1997). *Appl. Opt.* **36**, 1457.
Chrisp, M.P. (1983). *Appl. Opt.* **22**, 1519.
Ditmire, T. *et al.* (1996). *Phys. Rev. Lett.* **77**, 4756.
Glover, T.E. *et al.* (1996). *Phys. Rev. Lett.* **76**, 2468.
Harada, T. *et al.* (1999). *Appl. Opt.* **38**, 2743.
Kita, T. *et al.* (1983). *Appl. Opt.* **22**, 512.
Nakano, N. *et al.* (1984). *Appl. Opt.* **23**, 2386.
Nisoli, M. *et al.* (1996). *Appl. Phys. Lett.* **68**, 2793.
Nisoli, M. *et al.* (1997). *Opt. Lett.* **22**, 522.
Poletto, L. *et al.* (1999). *Proc. SPIE 3764*, 94.
Poletto, L. & Tondello, G. (2000). *Proc. SPIE 4138*, 182.
Poletto, L. *et al.* (2001). *Opt. Eng.* **40**, 178.
Priori, E. *et al.* (2000). *Phys. Rev. A* **61**, 063801.
Protopapas, M. *et al.* (1997). *Rep. Prog. Phys.* **60**, 389.
Salières, P. *et al.* (1998). In *Advances in atomic, molecular and optical physics*. Eds. B. Bederson, H. Walther (IOP, London).
Samson, J.A.R. & Ederer, D.L. (1998). *Vacuum ultraviolet spectroscopy II* (Academic Press, San Diego).
Spielmann, C. *et al.* (1997). *Science* **278**, 661.
Tondello, G. (1979). *Opt. Acta* **26**, 357.
Villoresi, P. *et al.* (2000). *Phys. Rev. Lett.* **85**, 2494.

https://doi.org/10.1017/S0263034601192050 Published online by Cambridge University Press